Quantum confinement of quasi-two-dimensional E_1 excitons in Ge nanocrystals studied by resonant Raman scattering

K. L. Teo,* S. H. Kwok, and P. Y. Yu†
Department of Physics, University of California, Berkeley, California
and Materials Sciences Division, Lawrence Berkeley National Laboratory, Berkeley, California 94720

Soumyendu Guha
Materials Science and Technology Division, Naval Research Laboratory, Washington DC 20375
(Received 8 November 1999)

Ge nanocrystals of diameters ranging from 4 to 10 nm were synthesized by ion implantation of Ge^+ ions into SiO_2 films followed by annealing. Confinement of its optical phonon and of the quasi-two-dimensional E_1 exciton have been observed at room temperature by resonant Raman scattering. The observed size-dependent blueshifts of the E_1 excitons energy (which can be larger than 0.7 eV) are found to be in good agreement with a theoretical calculation based on the effective mass approximation.

So far, there have been many reports of quantum confinements of electron-hole pairs (or excitons) in semiconductor nanocrystals (nc's). However, these efforts[1–3] have mainly been restricted to the study of the fundamental band gap only, while most semiconductors possess higher-energy excitons with quite large oscillator strengths. For example, the E_1 transitions in bulk Ge occur around 2.2 eV, well above the indirect and direct band gaps with energies of 0.6 and 0.9 eV, respectively.[4] So far, quantum confinement effects on the fundamental band gap in nc's have been explained theoretically[5–9] including the use of simple models like an infinite spherical well within the effective mass approximation.[10] However, there are relatively few calculations of the confinement effect on the higher-energy excitons for lack of experimental results. For probing transitions well above the fundamental gap, resonant Raman scattering (RRS) is superior to both absorption and emission, which are the standard techniques for studying confinement of excitons. In addition to electronic transitions, RRS can provide information on phonons and their interactions with electrons.[11] The latter capability is significant since it has been established that confinement effects can change the vibrational modes and hence the electron-phonon interaction of semiconductor nanostructures.[12–14] Recently, RRS has been applied to study the E_1 transitions in nm-size Ge quantum dots.[15,16] However, the confinement energy of the E_1 exciton for self-organized Ge quantum dots embedded in Si was found to be quite small.[16] In this paper we report a RRS study of the confinement of both the optical phonon and the E_1 exciton in Ge nc's embedded in the large-band-gap insulator SiO_2. We have been able to explain quantitatively the experimental results by using the effective mass approximation and by assuming the motion of the E_1 exciton to be *two dimensional*. This approximation is justified since the E_1 transitions involve electrons and holes along the [111] (or Λ) directions of the Brillouin zone where masses along the Λ directions are much larger than those perpendicular to the Λ directions.[17]

Nanocrystals of Ge were grown by implanting Ge^+ ions with kinetic energy of 190 keV into 500-nm-thick SiO_2 layers grown thermally on a Si wafer.[18] The implanted samples were annealed in a N_2 atmosphere at various temperatures up to 850 °C for 30 min followed by characterization with x-ray diffraction (XRD) and plane-view and cross-sectional high-resolution transmission electron microscopy (HRTEM). Sample characteristics obtained from these studies have already been detailed in Ref. 18. XRD indicates that, after annealing at around 800 °C, the nc's are crystalline and unstrained with the diffraction peaks appearing at the same positions as in bulk Ge. Examples of the XRD spectra of a sample before and after isochronal thermal annealing are shown in Fig. 1(a). In this paper we shall concentrate on three samples grown by implantation dosages of 1×10^{17}, 2×10^{17}, and 3×10^{17} ions/cm^2 and subsequently annealed at 800 °C. They will be referred to as Ge1, Ge2, and Ge3, respectively. Their nc-size distributions, as determined by HRTEM and reported in Ref. 18, can be fitted with either a log-normal or Gaussian function. The mean nc *diameters* are 4.2 and 6.5 nm for Ge1 and Ge2, respectively. The half-widths of these distributions are around 0.5–1 nm. From the broadening of the XRD peaks, we estimated the average nc diameters in Ge1, Ge2, and Ge3 to be 4, 7, and 10 nm (with uncertainties of ±1 nm), respectively.[19] Thus the average nc sizes determined by HRTEM and XRD measurements are in good agreement. The XRD spectra of Ge3 show a sharp peak in at $2\theta=26.5°$ [see Fig. 1(a)]. We tentatively identify this peak with GeO_2.[20] It was not seen in the XRD spectra of Ge1 and Ge2.

Raman spectra were measured in a near-backscattering geometry with a Spex Triplemate spectrometer and a cooled coupled channel device (CCD) array. The spectral resolutions of the spectrometer and the CCD pixel are 6 and 1 cm^{-1}, respectively. An Ar-ion pumped dye laser (with three different dyes: Stilbene 3, Coumarin 540, and Rhodamine 6G) was used to achieve a tuning range of 2.0–2.9 eV. All experiments were performed at room temperature. Although the Ge Raman peak was unpolarized, the Si substrate Raman peak was strongly polarized.[11] Thus it is important to ensure that the same scattering geometry was used in all the measurements.

 ©2000 The American Physical Society

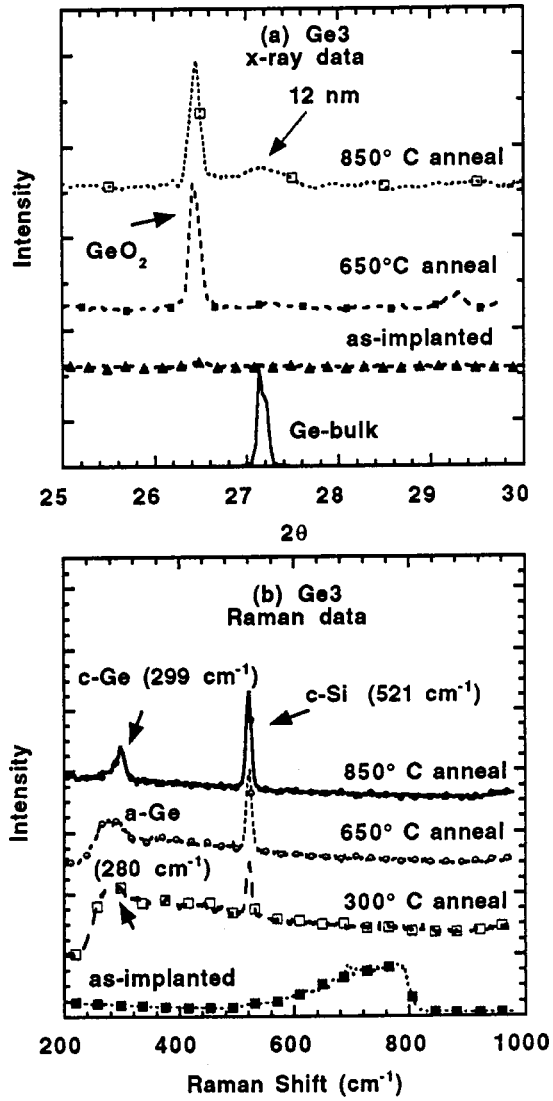

FIG. 1. (a) The x-ray and (b) Raman spectra of sample Ge3 as a function of annealing temperature.

Figure 1(b) shows some typical effects of annealing on the Raman spectra of implanted Ge samples (results are from Ge3 excited with a 2.71 eV laser). Three distinct features were (1) a sharp peak at 521 cm^{-1} due to the Si substrate (labeled as *c*-Si); (2) a broad and asymmetric peak centered around 299 cm^{-1}, which appeared after annealing at $\geqslant 800\,°C$, is identified as the one-phonon Raman mode of Ge nc's (labeled as *c*-Ge); and (3) a broadband around 280 cm^{-1} which appeared in samples annealed at $<800\,°C$, and probably contains contributions from an amorphous phase of Ge (Refs. 14 and 18) and (labeled as *a*-Ge) as well as some multiphonon modes of Si. Note that the optical phonon frequency in bulk Ge crystals is ~ 300 cm^{-1}.[11] The broadband around 700 cm^{-1} in the as-implanted sample may probably be due to oxygen vacancies created during the ion implantation.[21] Upon annealing, these defects were removed and this high-frequency band also disappeared.

In Fig. 2 we compare the line shapes of the Ge nc Raman peak in our three samples when excited by a laser of photon energy $\hbar\omega = 2.7$ eV. Notice that their width *increases* while their peak frequency *decreases* with a decrease in the nc's. Both effects have been observed before and analyzed in terms of the confinement of phonons.[14,22] The inset of Fig. 2 shows how the linewidth of Ge nc Raman peak varies with excitation photon energy. This result can be understood within the confinement models by including the effects of resonance enhancement and noting that our samples typically contain a distribution of nc sizes. At $\hbar\omega < 2.5$ eV the linewidth is relatively independent of $\hbar\omega$ because the Raman spectra are dominated by larger nc's whose phonons do not show strong confinement effects. At higher $\hbar\omega$ scattering from the smaller nc's becomes enhanced and the stronger confinement of their phonons results in a broadening of the Raman linewidth. In Ge2 and Ge3 where the linewidths are roughly independent of $\hbar\omega$, the average nc sizes deduced from the Raman linewidth using the model in Ref. 22 are consistent with the values obtained by XRD and HRTEM.

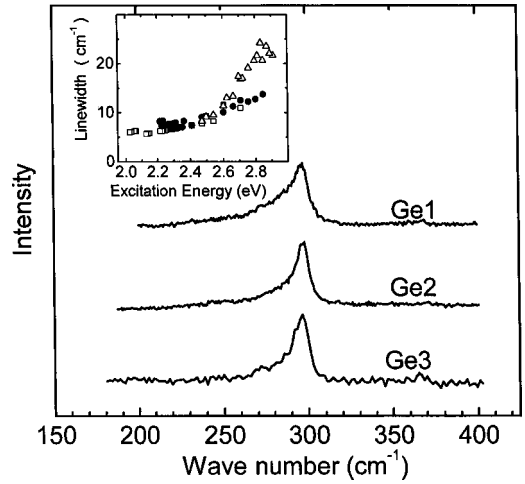

FIG. 2. The Ge Raman peak in the three Ge samples excited at $\hbar\omega = 2.7$ eV. The zeros of the three curves have been displaced vertically for clarity. The inset shows the change in the full width at half maximum of the Raman peak with laser energy for the three samples: Ge3 (open squares), Ge2 (solid circles), and Ge1 (open triangles).

To determine the dependence of the Ge nc Raman cross section on $\hbar\omega$, we first measured the Raman intensity of the Ge nc's *relative* to that of the Raman mode of the Si substrate. This intensity ratio is less sensitive to possible changes in optical alignment resulting from varying the dye laser wavelength. We then multiply this intensity ratio by the Raman cross section of Si at room temperature reported by Renucci *et al.*[23] The resulting cross sections for the three samples are shown as the data points in Fig. 3. The unit for the vertical axis in Fig. 3 is neither absolute nor completely arbitrary (although labeled so). This is because the Si Raman intensity we measured is not simply proportional to the Si Raman cross section. It depends on the absorption coefficient of Ge nc's in the SiO_2 layer since the incident and scattered radiation has to pass through this overlayer to reach the Si substrate. There is no simple way to determine the correction for this absorption effect without removing the Si substrate. In spite of this uncertainty, we do not expect the Ge absorption to change significantly the E_1 exciton peak energy as determined by RRS. We note that such absorption correction was found by Renucci *et al.*[24] to have little effect on the E_1 resonance energy determined by RRS in bulk Ge.

Consistent with our assumption, we found that the en-

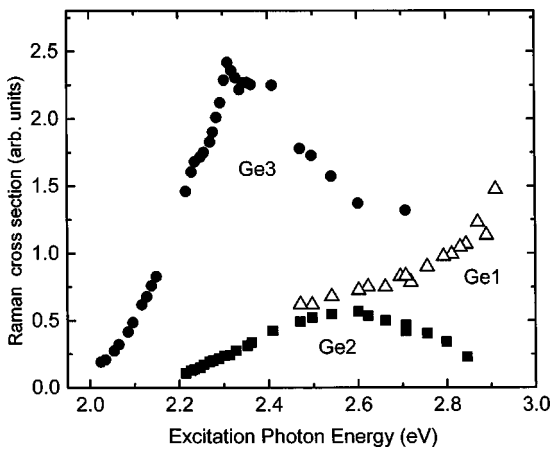

FIG. 3. The photon energy dependence of the Ge nc Raman cross section obtained by multiplying the measured ratios of the Ge to Si Raman intensities with the Si Raman cross section given in Ref. 24.

hancement peak in the Raman cross section in Ge3 occurs very close in energy to that of the E_1 and $E_1+\Delta_1$ transitions in bulk Ge (we shall neglect the spin-orbit splitting and refer to both transitions as the ''E_1 transitions'').[4] The width of the resonance in Ge3 is, however, larger due to the inhomogeneity in nc sizes. The peak in Ge3 is *blueshifted* from the E_1 transitions in bulk Ge by ~0.1 eV. This blueshift is considerably larger in Ge2 and for Ge1 the resonance is shifted to lie above our tuning range. We attribute these large nc-size-dependent blueshifts to quantum confinement effect on the energy of the E_1 exciton. So far, such an effect has been investigated theoretically in Ge only at the lowest indirect and direct band gaps.[1,5] However, the E_1 transitions involve electrons and holes along the Λ directions of the Brillouin zone and hence have quite different properties. For example, the electron and hole effective masses transverse to the Λ direction are much smaller ($<0.1m_0$, where m_0 is the free-electron mass) than the masses parallel to the Λ direction.[4] As a result, the E_1 excitons have been approximated as two-dimensional (2D) particles. To calculate the confinement energy of the E_1 excitons in Ge within the effective mass approximation, we further assume that the electron and hole confinement potentials are *infinite* and *spherical*. We first solve the Schrödinger equation for the motion of the 2D electrons and holes by neglecting their Coulomb attraction. The resultant wave functions are Bessel functions.[25] The Coulomb energy between the electron and hole is then calculated by perturbation theory using the 2D single-particle ground-state wave functions. The confinement energy of the 2D E_1 exciton obtained in this way is given by[25]

$$E_{x0}=\frac{\hbar^2}{2\mu_\perp}\left(\frac{2.405}{\rho}\right)^2-\frac{3.513e^2}{\varepsilon\rho}, \tag{1}$$

where $\hbar$ is the Planck constant, ρ is the nc *radius*, $\mu_\perp$ is the *reduced transverse* mass of the E_1 exciton in Ge ($=0.045m_0$),[17] e is the electric charge, and ε is the dielectric constant of the nc (assumed to be equal to 15.8, the same as in bulk Ge Ref. 4). Equation (1) is numerically different from the three-dimensional band gap excitons[1] because of the 2D nature of the E_1 exciton. For example, the Coulomb energy term in Eq. (1) is larger in 2D than in 3D. Figure 4 shows the confinement energy E_{X0} of the E_1 exciton as a function of ρ. The experimental values (solid circles) are obtained by subtracting the E_1 exciton energy in bulk Ge at room temperature (2.22 eV) from the resonance peak energies in Fig. 3. The resonance in Ge1 occurs at higher energy than we can reach with our dye laser so the experimental result is represented by a vertical bar. It is noteworthy that the good agreement between theory and experiment is achieved with no adjustable parameters in the theoretical calculation. This suggests that the simple effective mass approximation combined with a spherical infinite confinement potential works not only near the fundamental gap, but also at the higher-energy transitions.

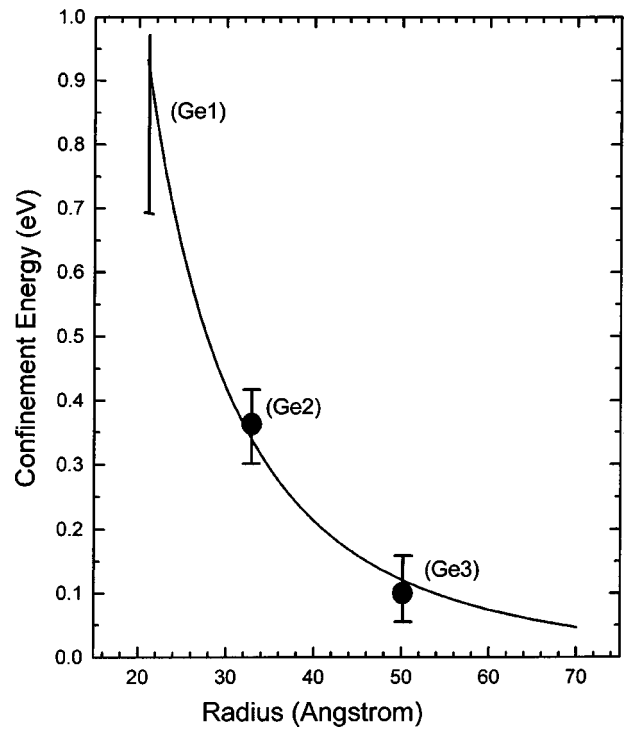

FIG. 4. The confinement energy of the E_1 exciton in Ge nc plotted as a function of radius. The solid line is the theoretical curve obtained from Eq. (1), while the solid circles and vertical bar are experimental results.

We note that the largest Raman cross section of Ge1 in Fig. 3 is almost as large as that of Ge3, although Ge1 contains 3 times *fewer* Ge atoms. This suggests that the Raman cross section *per Ge atom in* Ge1 must be *larger* than those of Ge3. This consideration does not include the correction for the reduction in the Si substrate Raman intensity by the Ge nc absorption which is expected to be larger in Ge3 than in Ge1. There have been many calculations[26–28] of the size dependence of exciton-phonon interaction in nc's. In general, long-range interactions such as the Fröhlich interaction and piezoelectric interaction are predicted to decrease with particle size. On the other hand, short-range interactions such as the deformation potential interaction are expected to be *enhanced with a decrease in particle size*. So far, this enhancement has been observed only for acoustic phonons in CdSSe nc's.[26] Our results suggest that enhancement also occurs for the optical phonons in Ge nc's.

In conclusion, we have observed via RRS confinement effects on both phonons and the E_1 exciton in Ge nc's grown by ion implantation in SiO_2. The measured exciton confinement energies are in quantitative agreement with a 2D model calculation using the effective mass approximation.

We acknowledge the following people for their help in this work. Randy Walker of Naval Research Laboratory for ion implantation, Mark Wall and Dominic Del Giudice of Lawrence Livermore National Laboratory (LLNL) for TEM and x-ray measurements. S.G. also appreciates Dr. L. L. Chase for an invitation to LLNL, where some of the work was done. The work at Berkeley was supported by the Director, Office of Energy Research, Office of Basic Energy Sciences, Materials Sciences Division, of the U.S. Department of Energy under Contract No. DE-AC03-76SF00098.

*Present address: Dept. of Electrical Engineering, National University of Singapore, Singapore 0511.

†Author to whom correspondence should be addressed. E-mail: PYYU@lbl.gov

[1] Y. Maeda, Phys. Rev. B **51**, 1658 (1995).

[2] D. J. Lockwood, Z. H. Lu, and J.-M. Baribeau, Phys. Rev. Lett. **76**, 539 (1996).

[3] T. van Buuren *et al.*, Phys. Rev. Lett. **80**, 3803 (1998).

[4] F. Cerdeira, W. Dreybrodt, and M. Cardona, Solid State Commun. **10**, 591 (1972); P. Y. Yu and M. Cardona, *Fundamentals of Semiconductors: Physics and Material Properties*, 2nd ed. (Springer-Verlag, Berlin, 1999), Chap. 6.

[5] Y. Kayanuma, Phys. Rev. B **38**, 9797 (1988); T. Takagahara and K. Takeda, *ibid.* **46**, 15 578 (1992).

[6] See, for example, L. Wang and A. Zunger, in *Nanocrystalline Semiconductor Materials*, edited by P. V. Kamat and D. Meisel (Elsevier Science, New York, 1996).

[7] N. A. Hill and K. B. Whaley, Phys. Rev. Lett. **75**, 1131 (1995); J. Electron. Mater. **25**, 269 (1996).

[8] S. Y. Ren, Solid State Commun. **102**, 479 (1997); Phys. Rev. B **55**, 4665 (1997).

[9] S. Ogut, J. R. Chelikowsky, and S. G. Louie, Phys. Rev. Lett. **79**, 1770 (1997); **83**, 1270 (1999).

[10] Al. L. Efros and A. L. Efros, Fiz. Tekh. Poluprovodn. **16**, 1209 (1982) [Sov. Phys. Semicond. **16**, 772 (1982)].

[11] See P. Y. Yu and M. Cardona, *Fundamentals of Semiconductors: Physics and Material Properties*, 2nd ed. (Springer-Verlag, Berlin, 1999), Chap. 7.

[12] P. M. Fauchet and I. H. Cambell, Crit. Rev. Solid State Mater. Sci. **14**, S79 (1988).

[13] C. E. Bottani *et al.*, Appl. Phys. Lett. **69**, 2409 (1996).

[14] T. Kobayashi *et al.*, Appl. Phys. Lett. **71**, 1195 (1997).

[15] Y. Sasaki and C. Horie, Phys. Rev. B **48**, 2009 (1993).

[16] S. H. Kwok *et al.*, Phys. Rev. B **59**, 4980 (1999).

[17] See M. L. Cohen and J. R. Chelikowsky, *Electronic Structure and Optical Properties of Semiconductors*, 2nd ed. (Springer-Verlag, Berlin, 1989), p. 95.

[18] S. Guha, M. Wall, and L. L. Chase, Nucl. Instrum. Methods Phys. Res. B **147**, 367 (1999).

[19] The Ge nc sizes measured in samples cut from different parts of the wafer may differ slightly. The sizes quoted in this article have been measured from the same chips where RRS was performed and differ slightly from those quoted in Ref. 18.

[20] M. Zacharias and P. M. Fauchet, Appl. Phys. Lett. **71**, 380 (1997).

[21] S. Guha, J. Appl. Phys. **84**, 5210 (1998).

[22] D. C. Paine *et al.*, Appl. Phys. Lett. **62**, 2842 (1993).

[23] J. B. Renucci, R. N. Tyte, and M. Cardona, Phys. Rev. B **11**, 3885 (1975).

[24] M. A. Renucci, J. B. Renucci and M. Cardona, in *Light Scattering in Solids*, edited by M. Balkanski (Flammarion, Paris, 1971), p. 326.

[25] See, for example, C. S. Johnson, Jr. and L. G. Pedersen, *Problems and Solutions in Quantum Chemistry and Physics* (Dover, New York, 1986), p. 122.

[26] See T. Takagahara, Phys. Rev. Lett. **71**, 3577 (1993) and references therein.

[27] P. A. Knipp and T. L. Reinecke, Phys. Rev. B **48**, 18 037 (1993).

[28] E. Roca, C. Trallero-Giner, and M. Cardona, Phys. Rev. B **49**, 13 704 (1994).